

Copyright WILEY-VCH Verlag GmbH & Co. KGaA, 69469 Weinheim, Germany, 2013.

## Supporting Information

### **Fabrication of Three-Dimensional Biomimetic Microfluidic Networks in Hydrogels**

*Keely A. Heintz, Michael E. Bregenzer, Jennifer L. Mantle, Kelvin H. Lee, Jennifer L. West, & John H. Slater\**

#### **Experimental Section**

*Preparation of PEGDA:* Poly(ethylene glycol) diacrylate (PEGDA) was prepared as previously described.<sup>[1]</sup> Briefly, 3350 Da PEG (Sigma-Aldrich) was dissolved in anhydrous dichloromethane (Sigma-Aldrich). Triethylamine (TEA; Sigma-Aldrich) and acryloyl chloride (ThermoFisher Scientific) were added dropwise at 1:2 (PEG:TEA) and 1:4 (PEG:acryloyl chloride) molar ratios. The solution was reacted under argon for 24 hr, washed with 1.5 M K<sub>2</sub>CO<sub>3</sub> (ThermoFisher Scientific), the aqueous and organic phases separated overnight, the organic phase dried with anhydrous MgSO<sub>4</sub> (ThermoFisher Scientific), and the PEGDA precipitated in diethyl ether (ThermoFisher Scientific). The PEGDA cake was sequentially air- and vacuum-dried for 24 hr each.

*Preparation of PEG-RGDS and Fluorescent PEG-RGDS:* Monoacrylate PEG-RGDS was prepared by reacting monoacrylate 3400 Da PEG-succinimidyl valerate (PEG-SVA; Laysan Bio) with RGDS (American Peptide) at a 1:1.1 molar ratio (PEG-SVA:RGDS) in anhydrous dimethyl sulfoxide (DMSO; Sigma-Aldrich) with anhydrous N,N-diisopropylethylamine (DIPEA; Sigma-Aldrich) at a 1:2 molar ratio (RGDS:DIPEA) for 24 hr.<sup>[2]</sup> To generate fluorescent PEG-RGDS, Alexa Fluor 633 succinimidyl ester (AF633; ThermoFisher Scientific) was added at a molar ratio of 50:1 (RGDS:AF633) in DMSO and reacted for an

additional 24 hr. For either product, the solution was added dropwise to ice cold deionized water (DI H<sub>2</sub>O) with a resistance of  $\geq 17.4 \text{ M}\Omega\text{-cm}$  obtained from a Neu-Ion high purity water filtration system (Neu-Ion Inc.) with an ultraviolet water disinfection system (Double Star Ultraviolet Systems). The solution was dialyzed in a regenerated cellulose membrane (Spectrum Labs) and lyophilized.

*Preparation of PDMS Molds:* Poly(dimethylsiloxane) (PDMS) spacers with a thickness of 300, 800, or 1500  $\mu\text{m}$  were created to define the shape and depth of reservoirs, and with a thickness of 500, 1000, and 2000  $\mu\text{m}$  to define the thickness and boundaries of the hydrogel, respectively. 1x38x75 mm glass slides (ThermoFisher Scientific) were treated with Sigmacote (Sigma-Aldrich) following the manufacturer's instructions. Two feeler gauges were clamped between two Sigmacote-treated slides, a well-mixed and degassed PDMS pre-polymer solution of 10:1 (base elastomer:curing agent) (Sylgard 184 Silicone Elastomer Kit; Dow Corning) was pipetted between the slides, and the assembly baked at 65 °C for 3 hr. The cured PDMS was removed from the slides and cut into desired shapes.

*Photopolymerization of Micromolded PEGDA:* 5% w/v PEGDA was photopolymerized under white light, for 3 min (500  $\mu\text{m}$  thick hydrogels), 10 min (800  $\mu\text{m}$  thick hydrogels), or 15 min (2000  $\mu\text{m}$  thick hydrogels) at 95  $\text{mW cm}^{-2}$ , via reaction of 3.4 kDa PEGDA in HEPES-buffered saline: pH 8.3, 10 mM HEPES (Sigma-Aldrich), 100 mM NaCl (Sigma-Aldrich), 1.5% triethanolamine (Sigma-Aldrich), with 3.5  $\mu\text{L mL}^{-1}$  1-vinyl-2-pyrrolidone (Sigma-Aldrich), and 10  $\mu\text{L mL}^{-1}$  1 mM eosin Y disodium salt (Sigma-Aldrich) in DIH<sub>2</sub>O between a PDMS mold and a [3-(Methacryloyloxy)propyl]trimethoxysilane (TMPSA; Sigma-Aldrich) functionalized glass coverslip to create 300  $\mu\text{m}$  deep reservoirs in a 500  $\mu\text{m}$  thick hydrogel (Figure 1). To impart free methacrylate groups on the glass for hydrogel coupling, 40 mm diameter, #1.5 glass coverslips (Warner Instruments) were cleaned with air plasma (Harrick

Plasma), functionalized for 24 hr in a 2% w/v solution of TMPSA in 190 proof ethanol (Decon Laboratories) with a pH of 4.5 adjusted with acetic acid (Sigma-Aldrich), and rinsed with 200 proof ethanol. Hydrogels were rinsed thoroughly with DI H<sub>2</sub>O for 48 hr to remove unreacted reagents.

*Virtual Mask Generation:* A 3D confocal image stack of cerebral cortex vasculature of a mouse was acquired as previously described<sup>[2]</sup> and graciously provided by Dr. Jim Culver and Dr. Mary Dickinson from the Baylor College of Medicine. A 3D computer-aided design (CAD) model of two independent yet intertwining microchannels was generated in SolidWorks (Dassault Systemes SolidWorks Corporation). The image features at each z-plane in the image stacks were converted to a mosaic of pixel wide, spatially defined regions of interest (ROIs) using custom-written algorithms in Matlab (The MathWorks Inc.).<sup>[2]</sup>

*PEGDA Degradation:* A custom-written routine in Zeiss MultiTime v16.0 (Carl Zeiss Inc.) utilized ROIs, either entered manually for simple geometries or defined by virtual masks for complex geometries,<sup>[2-5]</sup> to guide the position of a Chameleon Vision II (Coherent) 790 nm 140 fs pulsed Ti:S laser focused through a 20X(NA1.0) water immersion objective operating at a fluence of 21.7–37.7 nJ  $\mu\text{m}^{-2}$  using a Zeiss LSM 780 confocal microscope (Carl Zeiss Inc.) to induce hydrogel degradation. The laser scan speed was varied depending on the extent of hydrogel degradation desired. A slower scan speed, typically 0.021  $\mu\text{m} \mu\text{s}^{-1}$ , was used to create microchannels completely void of polymer, while a faster speed of up to 0.409  $\mu\text{m} \mu\text{s}^{-1}$ , depending on the amount of degradation desired, was used to create partially degraded microchannels. The pixel density of the view field was matched to the pixel density of the virtual masks to ensure optimal resolution. After degradation, the hydrogels were sonicated at for 10 min. To visualize degradation, 6 mM fluorescent PEG-RGDS was photocoupled to the hydrogel using the same reaction conditions described above to polymerize the PEGDA;

followed by thorough rinsing. Slight variations of this process were used to create the microfluidic channels and networks as described below.

*Fabrication and Visualization of Rectangular Microchannels:* A 500x100  $\mu\text{m}$  (x,y) rectangular ROI was created using the ROI function in ZEN Software (Carl Zeiss Inc.). The laser was stepped through the z-plane at 1  $\mu\text{m}$  intervals over 100  $\mu\text{m}$  resulting in 500x100x100  $\mu\text{m}$  (x,y,z) rectangular channels; a laser scan speed of 0.021  $\mu\text{m} \mu\text{s}^{-1}$  was used, with three passes at a constant fluence of 37.7  $\text{nJ} \mu\text{m}^{-2}$ . The processed hydrogel was sonicated and functionalized with 6 mM fluorescent PEG-RGDS as described in the previous section. The fluorescent PEG-RGDS was imaged with a 20X(NA0.8) objective using a Zeiss LSM 780 inverted confocal microscope (Carl Zeiss Inc.). The reservoir feeding the microchannels was filled with 5  $\mu\text{L}$  of solution containing 1  $\text{mg mL}^{-1}$  2000 kDa tetramethylrhodamine (TRITC)-labeled dextran (ThermoFisher Scientific), 1  $\text{mg mL}^{-1}$  500 kDa fluorescein (FITC)-labeled dextran (ThermoFisher Scientific), and 1  $\text{mg mL}^{-1}$  10 kDa Cascade Blue-labeled dextran (ThermoFisher Scientific). The fluorescence from the three dextrans was imaged after 20 min, and the reservoir and microchannels rinsed thoroughly with DI  $\text{H}_2\text{O}$ . The reservoir was refilled with 5  $\mu\text{L}$  of solution containing yellow-green 200 nm and Nile Red 2  $\mu\text{m}$  diameter fluorescent latex spheres (ThermoFisher Scientific) and imaged again. A 3D rendering of the hydrogel and fluorescent species in the microchannels was generated using the *Volume Viewer* plugin in Fiji (NIH).

*Fabrication, Visualization, and Characterization of Partially Degraded Microchannels:* 300x15x15  $\mu\text{m}$  (x,y,z) microchannels were fabricated as described in the previous section using 8 different laser scan speeds (0.005-0.409  $\mu\text{m} \mu\text{s}^{-1}$ ), five subsequent passes of the laser at a constant fluence of 21.7  $\text{nJ} \mu\text{m}^{-2}$ , and a z-spacing of 1  $\mu\text{m}$ . The hydrogels were sonicated and functionalized with fluorescent PEG-RGDS as described above. The eosin Y and

fluorescent PEG-RGDS were imaged with a 25X(NA0.8) water immersion objective using a Zeiss LSM 710 inverted confocal microscope (Carl Zeiss Inc.) equipped with an incubation chamber set to 60% humidity and 22 °C. The reservoir was filled with 5  $\mu\text{L}$  of solution containing 0.5  $\text{mg mL}^{-1}$  2000 kDa FITC-labeled dextran (ThermoFisher Scientific) and 0.5  $\text{mg mL}^{-1}$  10 kDa TRITC-labeled dextran (ThermoFisher Scientific), the fluorescent species given 30 min to perfuse, and the hydrogel imaged again. Intensity measurements in the x-direction (averaged in the y-direction) were acquired in the region depicted by the dashed white rectangle (Figure 2A) using Fiji (NIH). The background signals for the 10 kDa and 2000 kDa dextran were subtracted from the intensity measurements and the values normalized to the highest signal for each fluorophore.

*Size-Based Separation of Fluorescent Biomolecules Using Microchannels with a Linear Degradation Gradient:* A prefabricated microfluidic device consisting of six parallel channels all 17x3.8x0.4 mm (x,y,z), backed with adhesive (Sticky-Slide VI<sup>0.4</sup> luer microscopy chamber; Ibidi), was attached to a TMPSA-treated 25x75 mm #1.5 thickness coverglass (Ibidi). One of the channels was filled with 1 mM eosin Y solution, as described above, incubated for 30 min at room temperature, and dried with  $\text{N}_2$ . 5% 3.4 kDa PEGDA prepolymer solution, as described above, was pumped into the channel using a syringe. Using a photomask, the prepolymer solution was photopolymerized in the channel resulting in a 1x3.8x0.54 mm (x,y,z) hydrogel that was thicker than the channel height due to the adhesive layer. After rinsing with DI  $\text{H}_2\text{O}$  for 3 days, a 20  $\mu\text{m}$  square channel was degraded through the center of the 1 mm wide hydrogel with the same laser parameters used to generate the partially degraded microchannels (Figure 2A); the laser scan speed was increased in a gradient fashion from 0.005 to 0.409  $\mu\text{m } \mu\text{s}^{-1}$  in the x-direction to create a microchannel with a linear gradient in the amount of hydrogel degraded. A syringe pump (PHD 22/2000; Harvard Apparatus) was used to flow a solution containing 0.1  $\text{mg mL}^{-1}$  2000 kDa FITC-labeled

dextran (ThermoFisher Scientific), 0.1 mg mL<sup>-1</sup> 10 kDa TRITC-labeled dextran (ThermoFisher Scientific), and blue 2 μm diameter fluorescent polystyrene spheres (ThermoFisher Scientific) at 10 μL min<sup>-1</sup> into the microfluidic device. The fluorescent species were imaged with a 10X(NA0.3) objective using a Zeiss AxioObserver Z1 microscope (Carl Zeiss Inc.).

*Fabrication and Visualization of Vascular-Derived, Biomimetic Microfluidic Networks:* A custom-written routine in ZEN MultiTime v16.0 (Carl Zeiss Inc.) utilized the coordinates defined by the virtual masks generated from the cerebral cortex vasculature image stack<sup>[2]</sup> to guide the laser position<sup>[3-5]</sup> during degradation; a laser scan speed of 0.021 μm μs<sup>-1</sup> was used, with one pass of the laser at a constant fluence of 37.7 nJ μm<sup>-2</sup>. The vascular-derived biomimetic microfluidic networks were fabricated using 30 virtual masks, each derived from one z-plane image of the cerebral cortex vasculature.<sup>[2]</sup> Each of the 30 virtual masks was utilized three times with a z-spacing of 0.95 μm (to match the voxel depth of the cerebral cortex vasculature image stack, 2.84 μm) for a total depth of 85.5 μm. A 40x40 μm (y,z) channel connecting the reservoir to the vascular-derived network was created to introduce flow. To visualize the vascular-derived, biomimetic microfluidic networks, the reservoir was filled with 5 μL of 1 mg mL<sup>-1</sup> 2000 kDa FITC-labeled dextran (ThermoFisher Scientific), the dextran given 30 min to diffuse, and the 3D microfluidic network imaged with a 25X(NA0.8) water immersion objective using a Zeiss LSM 710 inverted confocal microscope (Carl Zeiss Inc.) equipped with an incubation chamber set to 60% humidity and 22 °C (Figure 3A). Three vascular-derived microfluidic networks were fabricated, imaged, and characterized as described in the following section.

*Characterization of Vascular-Derived Biomimetic Microfluidic Networks:* Skeletonization and quantification of branching nodes, terminal nodes, and total network length of each

vascular network was performed using AMIRA 3D Software for Life Sciences (FEI Visualization Sciences Group). The analysis was applied to the cerebral cortex vasculature image stack used to derive the biomimetic microfluidic network, and to image stacks of the three photodegraded vascular-derived microfluidic networks for direct comparison. Each vascular structure was defined by creating a label image object using the *Edit New Label Field* function followed by thresholding using the *Segmentation Editor*. A 3D polygonal surface model of the vasculature was created using the *Generate Surface* module. To obtain branching node, terminal node, and network length data, skeletons of the vascular networks were created using *Distance Map*, *Thinner*, and *Trace Lines* modules sequentially. A threshold of 9 voxels (Len of Ends = 9) was used for thinning to eliminate terminal nodes with lengths smaller than 9 voxels to minimize sensitivity to surface roughness. The *Trace Lines* module was attached to the thinned data object to generate a spatial graph object to view nodes and segments. Due to the complexity of the vascular networks, the *Filament Editor* was used to manually edit errant nodes by extending the position of terminal nodes, consolidating closely positioned branching nodes, adding missing nodes and segments, and deleting erroneous nodes and segments. The skeleton was smoothed with a point averaging algorithm using the *Smooth Line Set* module. A *Spatial Graph Statistics* module was attached to the resultant *SmoothTree* object to measure the number of branching nodes, terminal nodes, and the total network length. The vessel diameters were measured in Fiji (NIH) by overlaying a 5x5 grid on each image stack as a reference field and choosing five vessels in each box to measure. A total of 125 vessel diameter measurements were acquired for the same vessels in each image stack.

*Statistical Analysis Comparing In Vivo to Vascular-Derived Microfluidic Networks:* Statistical analysis of branching nodes, terminal nodes, total network length, and vessel diameter were presented as mean  $\pm$  standard deviation (Figure 3B) and were analyzed using a two-tailed t-test for populations with unknown variance assuming a normal distribution.

Unknown variance was used since only an n of one existed for the original *in vivo* vascular image. The absolute value of the calculated test statistic was compared to the critical value corresponding to a significance level  $\alpha = 0.05$ . Differences were considered to be statistically significant if the absolute value of the test statistic was greater than the critical value.

*Cell Culture, Fluorescent Labeling, and Imaging in Microchannels:* 50  $\mu\text{m}$  diameter circular channels were degraded using 25 virtual masks, each utilized two times due to the symmetry of the channel, with a z-spacing of 1  $\mu\text{m}$ . The microchannels were degraded through the PEGDA, from one reservoir to the other, to connect the two reservoirs together; a laser scan speed of 0.021  $\mu\text{m} \mu\text{s}^{-1}$  was used, with one pass at a constant fluence of 37.7  $\text{nJ} \mu\text{m}^{-2}$ . The degraded hydrogels were sonicated and functionalized with 6 mM PEG-RGDS as described above. Hydrogels were rinsed once with 70% ethanol for 30 min and 3x with sterile phosphate buffered saline (Sigma-Aldrich) for 24 hr. Cells from a mouse brain endothelial cell line (bEnd.3; ATCC) were cultured at 37 °C and 5%  $\text{CO}_2$  in complete medium, consisting of Dulbecco's Modified Eagle's Medium (DMEM; ATCC) supplemented with 10% fetal bovine serum (FBS; ThermoFisher Scientific) and 1% antibiotic-antimycotic (Streptomycin, Penicillin, Amphotericin B; ThermoFisher Scientific) in a T-25 flask until 90% confluence. Cells were trypsinized (Corning), centrifuged at 250 g for 6 min, and resuspended in complete medium. A pressure head was created in one reservoir to flow the cell suspension through the microchannels connecting the two reservoirs. Cells were allowed to adhere to the microchannel walls for 8 hr before 6 mL of complete medium was added to the Petri dish. Cells were statically cultured using complete medium with exchanges every 3 days. After 11 days, cells were fluorescently labeled to visualize cell nuclei (DAPI) and zona occludens protein 1 (ZO-1) indicating tight junctions. All immunocytochemistry solutions were prepared in Dulbecco's phosphate-buffered saline (DPBS; ThermoFisher Scientific) unless otherwise specified. Briefly, cells were rinsed 2x with cold DPBS, fixed for 15 min in



2% paraformaldehyde (Electron Microscopy Sciences), rinsed 3x with DPBS, permeabilized with 0.1% Triton X-100 (Sigma-Aldrich) for 5 min, blocked with 10% goat serum (Sigma-Aldrich) for 1 hr, and incubated with 1  $\mu\text{g mL}^{-1}$  rabbit anti-ZO1 polyclonal antibody (ThermoFisher Scientific) in 10% goat serum for 12 hr at 4°C. The samples were rinsed 3x with DPBS and incubated with 4  $\mu\text{g mL}^{-1}$  Alexa Fluor 488 conjugated goat anti-rabbit antibody (ThermoFisher Scientific) in 10% goat serum for 1.5 hr, washed 3x with DPBS, and incubated with 300 nM DAPI (ThermoFisher Scientific) for 10 min followed by rinsing 3x with DPBS. Cells were imaged with a 20X(NA0.8) objective using a Zeiss LSM 710 inverted confocal microscope (Carl Zeiss Inc.). 3D renderings of the fluorescently labeled cells in the microchannels were generated using the *Volume Viewer* plugin in Fiji (NIH).

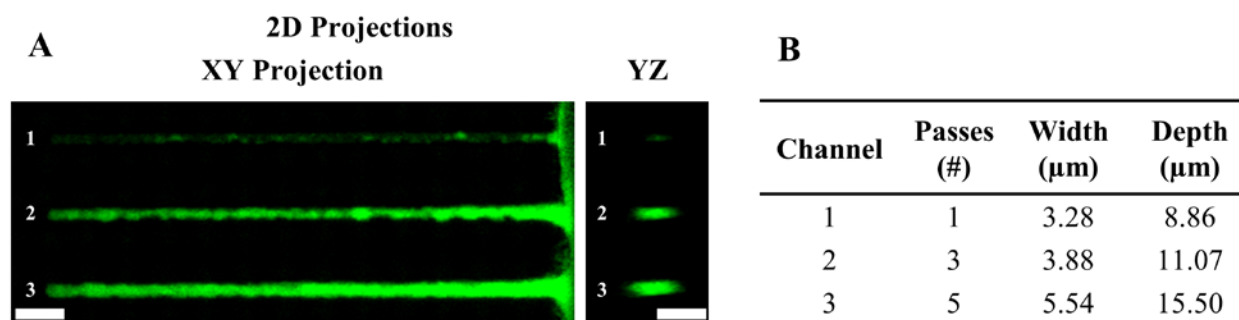
*Fabrication, Visualization, and Characterization of Intertwining Microchannels:* Seven virtual masks generated from the SolidWorks model were used ten times each, at a z-spacing of 2  $\mu\text{m}$ , to fabricate the intertwining microchannels; a laser scan speed of 0.021  $\mu\text{m } \mu\text{s}^{-1}$  was used, with two passes at a constant fluence of 37.7  $\text{nJ } \mu\text{m}^{-2}$ . The degradation was performed twice to account for the increased spacing between masks followed by sonication and rinsing. To visualize the intertwining microchannels, one reservoir was filled with 5  $\mu\text{L}$  of 1  $\text{mg mL}^{-1}$  AF488-labeled BSA (ThermoFisher Scientific) and the other with 1  $\text{mg mL}^{-1}$  TRITC-labeled 70 kDa dextran (ThermoFisher Scientific). The species were given 30 min to perfuse into the networks, and imaged with a 25X(NA0.8) water immersion objective using a Zeiss LSM 710 inverted confocal microscope (Figure 4B). A 3D rendering was generated using the *Volume Viewer* plug-in in Fiji (NIH) (Figure 4B). To quantify transport along and between the intertwining microchannels, one reservoir was filled with 5  $\mu\text{L}$  of 1  $\text{mg mL}^{-1}$  AF594-labeled BSA (ThermoFisher Scientific), the other with 1  $\text{mg mL}^{-1}$  2000 kDa FITC-labeled dextran (ThermoFisher Scientific), and time-lapse confocal images were acquired at 5 min intervals for 2 hr with a 10X(NA0.3) objective using the same microscope and incubator chamber

settings as mentioned in a previous section. Average intensity values were obtained from the region indicated by the white rectangles (Figure 4C). To ensure that reported time-lapse intensity profiles were due primarily to species movement between microchannels, background intensity values were obtained from a region equidistant from each of the reservoirs as the white rectangles (Figure 4C) and subtracted at each time point. The measured intensity values for each fluorescent species were normalized to their highest value measured in the time-lapse images within their own channel. The experiment was performed in triplicate to determine the average and standard deviation.

*Fabrication and Visualization of Microchannels at Various Depths:* PDMS molds were used to fabricate thicker hydrogels with deeper reservoirs, namely a 1000  $\mu\text{m}$  thick hydrogel with an 800  $\mu\text{m}$  deep reservoir, and a 2000  $\mu\text{m}$  thick hydrogel with a 1500  $\mu\text{m}$  deep reservoir. A 200x15  $\mu\text{m}$  (x,y) rectangular ROI was created using the ROI function in ZEN Software (Carl Zeiss Inc.). The laser was stepped through the z-plane at 1  $\mu\text{m}$  intervals over 15  $\mu\text{m}$  resulting in 200x15x15  $\mu\text{m}$  (x,y,z) rectangular channels; a laser scan speed of 0.005  $\mu\text{m} \mu\text{s}^{-1}$  was used, with one pass at a constant fluence of 37.7  $\text{nJ} \mu\text{m}^{-2}$ . Channels were successively degraded 100 or 150  $\mu\text{m}$  apart from each other in the 800  $\mu\text{m}$  or 1500  $\mu\text{m}$  deep reservoirs, respectively. The processed hydrogels were sonicated for 10 min. The reservoirs were filled with 1  $\text{mg mL}^{-1}$  2000 kDa FITC-labeled dextran (ThermoFisher Scientific), the dextran given 30 min to diffuse, and the samples images with a 10X(NA0.3) objective using a Zeiss LSM 710 inverted confocal microscope (Carl Zeiss Inc.) equipped with an incubation chamber set to 60% humidity and 22  $^{\circ}\text{C}$ . Max intensity z-projections and orthogonal views of the dextran in the microchannels were generated using Fiji (NIH); a 3D rendering was generated using the *Volume Viewer* plugin of Fiji.

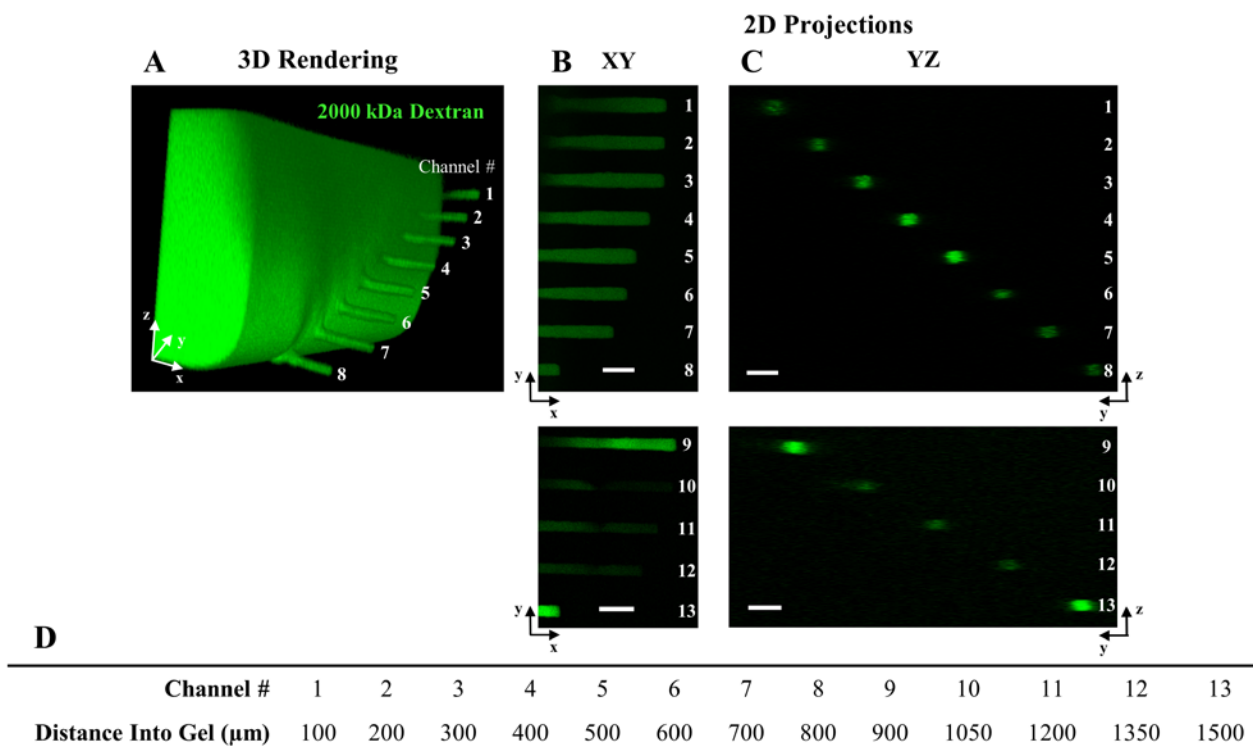
*Fabrication, Visualization, and Characterization of Resolution Microchannels: A 200x3.68  $\mu\text{m}$  (x,y) rectangular ROI was created using the ROI function in ZEN Software (Carl Zeiss Inc.). The laser was scanned at two z-planes spaced by 1  $\mu\text{m}$ . A laser scan speed of 0.010  $\mu\text{m} \mu\text{s}^{-1}$  was used, with 1, 3, or 5 passes at a constant fluence of 37.7  $\text{nJ} \mu\text{m}^{-2}$ . The processed hydrogels were sonicated for 10 min. The reservoir was filled with 1  $\text{mg mL}^{-1}$  2000 kDa FITC-labeled dextran (ThermoFisher Scientific), the dextran given 30 min to diffuse, and the microchannels imaged with a 25X(NA0.8) water immersion objective using a Zeiss LSM 710 inverted confocal microscope (Carl Zeiss Inc.) equipped with an incubation chamber as mentioned previously. Max intensity z-projections and orthogonal views of the dextran in the microchannels were generated using Fiji (NIH). Channel widths and depths were measured in Fiji using the full width at half maximum of line scan intensity profiles.*

*Fabrication, Visualization, and Characterization of Diffusion at the Degradation Interface: A 200x500  $\mu\text{m}$  (x,y) rectangular ROI was created using the ROI function in ZEN Software (Carl Zeiss Inc.), in order to remove a 200x500  $\mu\text{m}$  (x,y) region from the wall of the hydrogel reservoir. The laser was scanned at 21 z-planes spaced by 2  $\mu\text{m}$ , centered 150  $\mu\text{m}$  below the surface of the hydrogel for total removal of a 200x500x40  $\mu\text{m}$  (x,y,z) region. A laser scan speed of 0.010  $\mu\text{m} \mu\text{s}^{-1}$  was used, with a single pass at a constant fluence of 37.7  $\text{nJ} \mu\text{m}^{-2}$ . The processed hydrogel was sonicated for 10 min. The reservoir feeding the microchannels was filled with 5  $\text{mg mL}^{-1}$  10 kDa FITC-labeled dextran (Sigma Aldrich). The diffusion of dextran into the degraded edge of the hydrogel was imaged after 45 minutes with a 25X(NA0.8) water immersion objective using a Zeiss LSM 710 inverted confocal microscope (Carl Zeiss Inc.) equipped with an incubation chamber as mentioned previously. Line scan intensity profiles of 4.6  $\mu\text{m}$  width were recorded using Fiji (NIH).*



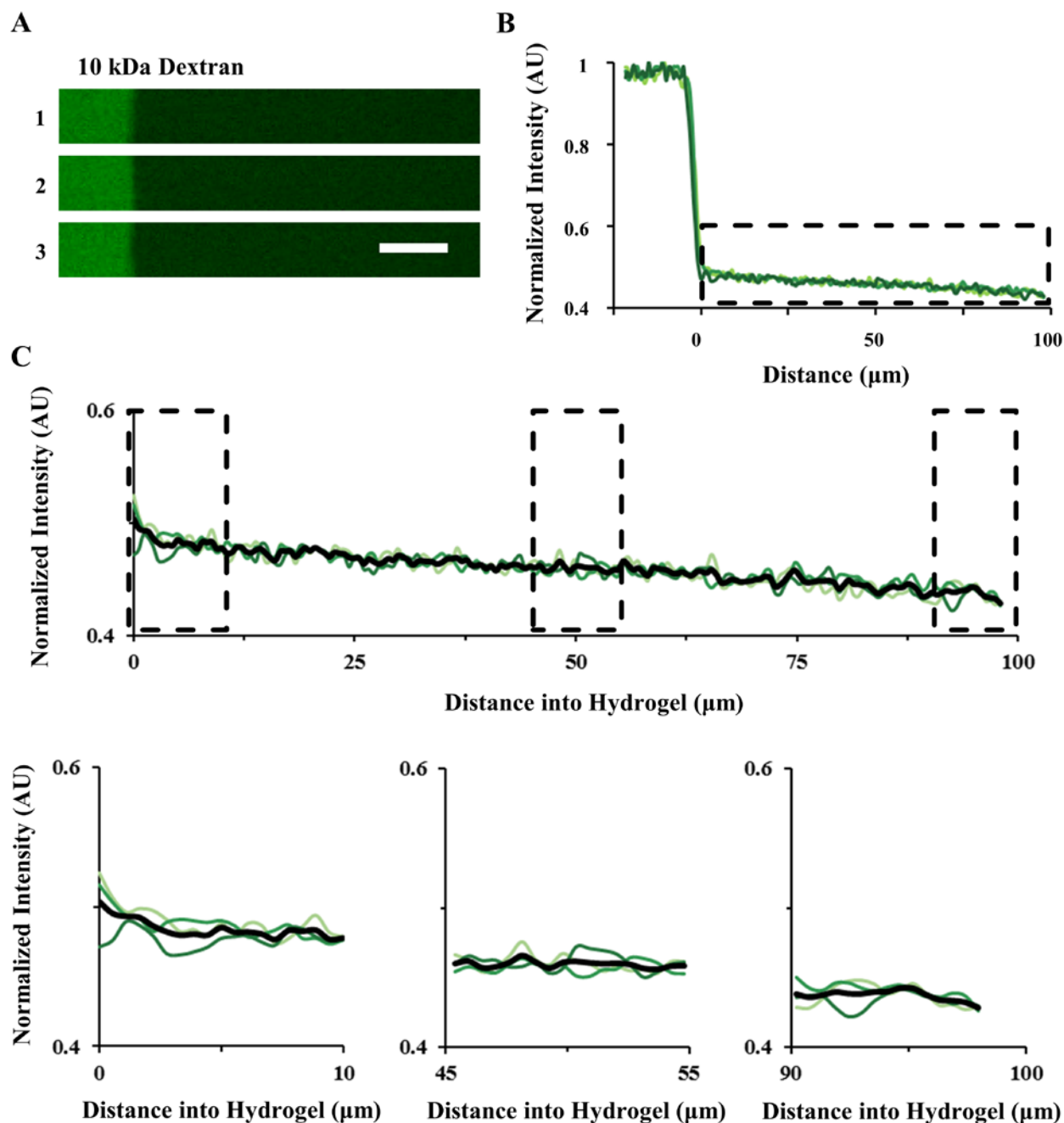
**Supplemental Figure 1: Microchannel Size as a Function of Number of Passes**

(A) A z-projection and orthogonal YZ-plane depicting three microchannels perfused with (green) 2000 kDa dextran fabricated using a 790 nm laser operating at  $37.7 \text{ nJ } \mu\text{m}^{-2}$  with a scan speed of  $0.010 \text{ } \mu\text{m } \mu\text{s}^{-1}$ . The number of times the laser was scanned over the same volume was varied (1, 3 or 5 passes) to generate microchannels 1-3 respectively. (B) The microchannel width and depth as a function of the number of passes was measured. The smallest channel generated with these parameters had a width of  $3.28 \text{ } \mu\text{m}$  and a depth of  $8.86 \text{ } \mu\text{m}$ . (A,B) SB= $20 \text{ } \mu\text{m}$ .



### Supplemental Figure 2: Fabrication of Microchannels at Varying Depths

(A) A 3D rendering of microchannels filled with (green) fluorescently labeled 2000 kDa dextran extending from a micromolded well into a PEGDA hydrogel. Eight  $200 \times 15 \times 15 \mu\text{m}$  ( $x, y, z$ ) channels extending from the well into the hydrogel were fabricated at varying depths (100–800  $\mu\text{m}$ ), perfused with (green) fluorescent 2000 kDa dextran, and imaged via confocal microscopy. (B) Z-projections and (C) orthogonal YZ-planes of microchannels 1–8 extending from a 800  $\mu\text{m}$  deep well, and channels 9–13 extending from a 1500  $\mu\text{m}$  deep well, demonstrate that hydrogel degradation can occur at depths of up to 1500  $\mu\text{m}$ ; degradation up to the working distance of the 20X(NA1.0) water immersion objective, 1800  $\mu\text{m}$ , was not tested. (D) Distances of each of the channels from the tops of the two hydrogels (in the  $z$ -direction) are listed. (B,C) SB=50  $\mu\text{m}$ .



### Supplemental Figure 3: Diffusion of Dextran into PEGDA at Degradation Interface

(A) A large volume of PEGDA was degraded to form a reservoir and filled with (green) fluorescently labeled 10 kDa dextran. Diffusion of the dextran from the degraded reservoir into the hydrogel was imaged after 45 min with confocal microscopy ( $n=3$ ). (B) Normalized intensity profiles of the 10 kDa dextran in the reservoir and in the hydrogel, with the interface set at zero, show a leveling off of dextran from the degraded edge into the bulk material (dashed black box). (C) Looking more closely at the hydrogel region, this leveling off of the fluorescent signal shows that the material at the interface is characteristic of the bulk material, and that the degradation is primarily confined to the scanned regions. (C: bottom left) Over a 1.1  $\mu\text{m}$  distance from the interface into the hydrogel, we observed a change in the slope of the intensity from 0.5039 to 0.4932. This relates to a 1.0653% increase in intensity directly adjacent to the interface, which would indicate that the hydrogel at the interface may be slightly degraded. We should emphasize that a 1.06% increase in intensity across a short 1.1

$\mu\text{m}$  distance indicates that there is very little degradation outside of the scanned region, but that some does occur. (A) SB=20  $\mu\text{m}$ .

## References

- [1] S. A. DeLong, A. S. Gobin, J. L. West, *J. Controlled Release* **2005**, *109*, 139.
- [2] J. C. Culver, J. C. Hoffmann, R. A. Poché, J. H. Slater, J. L. West, M. E. Dickinson, *Adv. Mater.* **2012**, *24*, 2344.
- [3] J. H. Slater, J. C. Culver, B. L. Long, C. W. Hu, J. Hu, T. F. Birk, A. A. Qutub, M. E. Dickinson, J. L. West, *ACS Nano* **2015**, *9*, 6128.
- [4] A. Shukla, J. H. Slater, J. C. Culver, M. E. Dickinson, J. L. West, *ACS Appl. Mater. Interfaces* **2015**, DOI 10.1021/acsami.5b08978.
- [5] J. H. Slater, J. L. West, in *Methods Cell Biol.*, Elsevier, **2014**, pp. 193–217.